Journal of Sound and Vibration (1997) **206**(2), 151–168

LARGE AMPLITUDE FREE VIBRATIONS OF A UNIFORM CANTILEVER BEAM CARRYING AN INTERMEDIATE LUMPED MASS AND ROTARY INERTIA

M. N. Hamdan and M. H. F. Dado

Mechanical Engineering Department, University of Jordan, Amman, Jordan

(*Received* 3 *April* 1996, *and in final form* 5 *March* 1997)

This work is concerned with the non-linear period, for each of the first four modes, of planar, flexural large amplitude free vibrations of a slender, inextensible cantilever beam carrying a lumped mass with rotary inertia at an intermediate position along its span. Following the analysis carried out in reference [1] on a similar class of beam system, the shear deformation and rotary inertia are assumed to be negligible, while account is taken of axial inertia, non-linear curvature and the inextensibility condition, and an assumed single-mode Lagrangian method is used to form directly the third order non-linear unimodal temporal problem. Because of the strong non-linear terms in the temporal problem, the two-term harmonic balance (2THB) method is used to obtain an approximate solution to the period of oscillation. The 2THB results are compared, for some selected values of sytem parameters, to those obtained by using single term harmonic balance (STHB) and to those obtained by numerical integration of the temporal problem. Results in non-dimensional forms are presented graphically, for each of the first four modes, for the effect of position and magnitude of the mass and rotary inertia of the attached element on the variation of period of oscillation with amplitude.

1. INTRODUCTION

Many engineering structures can be modelled as a slender, flexible cantilever beam carrying a lumped mass with rotary inertia at an intermediate point along its span. In linear theory analysis of vibration one assumes the frequency of free vibration of such a beam system to be independent of motion amplitude and this is valid only when the motion amplitude is kept relatively small. Such beam systems, however, being slender and flexible, often undergo relatively large amplitude (i.e., peak amplitudes on the order of beam length at the lower modes) flexural vibration—as, for example, in the neighbourhood of direct or parametric resonance frequencies [2–4], where non-linear effects no longer can be ignored. In such cases, and in forced vibration of non-linear system in general, it is of interest to know the free vibration frequency–amplitude relation as this relation enables one to establish the qualitative behavior, i.e., it defines the "backbone" curve, of the steady state forced response.

The problems of non-linear free and forced vibrations of beam have received considerable attention in the past few decades. Comprehensive reviews on this subject have been presented, e.g., by Rosenberg [5], Eisley [6], Nayfeh and Mook [7], and Sathyamoorthy [8,9], among others. A review on works on the subject is not provided herein; instead, the reader is referred to a recent summary [1] of the relevant literature on

0022–460X/97/370151 + 18 $25.00/0/sv971081

the large amplitude free vibration of beams with inertia and/or geometric non-linear effects.

In the present work the non-linear, large amplitude free vibrations of a slender, inextensible cantilever beam carrying a lumped mass and rotary inertia at an intermediate position along its span are considered. Here, the meaning of "large " implies that the peak amplitude may reach a value where the non-linear terms are of an order comparable to that of the linear ones. For example, the peak amplitude, for the lower nodes, may be of the order of beam length; i.e., it is not restricted to the order of beam thickness. The shear deformation and rotary inertia effects of the beam are assumed to be negligible, and the beam is assumed to be undergoing planar flexural vibrations. With account taken of axial inertia, non-linear curvature and the inextensibilty condition, an assumed Galerkin, single-linear mode, Lagrangian approach is used to form directly the third order non-linear unimodal temporal problem. The assumed deflection for each mode used in this work is the exact linear mode shape obtained by solving the associated linear problem which takes into account the effect of the attached lumped mass and rotary inertia. Because of the presence of the intermediate rotary inertia and lumped mass, solving the associated linear problem, i.e., solving the transcendental frequency equation of the linear problem and finding the linear mode shapes, becomes rather involved algebraically. Furthermore, the coefficients in the discrete single mode temporal problem are evaluated from integrals involving products of the assumed mode and its derivatives. To simplify the algebra, one may select a mode shape which satisfies the boundary condition of the linear problem but which does not take into account the effect of the attached rotary inertia and/or lumped mass. For example, Zavodney and Nayfeh [2] selected a linear mode shape to discretize a parametrically excited slender, flexible cantilever beam carrying a rotary inertia and a lumped mass, which takes into account the effect of the lumped mass but not the effect of the attached rotary inertia. Hamdan and Shabaheh [1] used the mode shape of the base beam (the same beam but without the attached elements) to discretize a non-linear beam similar to the one under consideration which carries only a lumped mass. The effect of using approximate mode shapes on the period–amplitude behavior will be discussed in the current work.

Because of the strong non-linear terms in the temporal problem, a first order approximate solution obtained by using the small perturbation method or a STHB procedure may fail to yield the correct qualitative period–amplitude behavior when the amplitude of motion becomes relatively large [10]. It is noted that several method have been used to obtain approximate solutions for both weakly and strongly non-linear oscillators; a review of relevant literature on this subject may be found in, e.g., reference [10]. In the harmonic balance (HB) method, the more widely used of these methods, a periodic solution for the dependent variable is assumed in the form of a Fourier series, mostly truncated to only a few leading harmonics. In order to improve accuracy, one increases the number of the retained leading harmonics in the assumed series solution. Recently, Hamdan and Shabaneh [10], analyzed the free vibration period–amplitude behavior of a generalized version of the strongly non-linear temporal problem considered in this work. They showed that the application of the HB method in which only the two leading harmonics are retained, termed herein the 2THB method, yields reasonably accurate results over a wide range of system parameters. Based on these results, and because of its generality and common use, the 2THB method is chosen in the current work to obtain an approximate solution to the period of free oscillation of the strongly non-linear temporal problem. Results in non-dimensional forms, for each of the first four modes, are presented graphically for the effects of position and magnitude of the intermediate lumped mass and rotary inertia on the variation of period of oscillation with

amplitude. Comparisons of the 2THB results with those of the first order approximations obtained by using STHB, as well as with those obtained by numerical integration of the temporal problem, are presented for some selected values of system parameters. The emphasis of this work is on the large amplitude motions where the non-linear terms may be of order comparable to that of the linear ones. Hamdan and Latif [11], and others (see, e.g., reference [12]) have presented parametric studies on the effects of attached inertia elements on the natural frequencies of relevant linear problems. Studies of relevant non-linear problems, however, are less abundant.

2. ASSUMPTIONS AND EQUATION OF MOTION

2.1. SYSTEM DESCRIPTION AND ASSUMPTIONS

A schematic of the beam under study is shown in Figure 1. The beam is considered to be uniform of constant length l and mass m per unit length, clamped at the base, free at the tip, and carries a lumped mass M and rotary inertia J at an arbitrary intermediate point $s = d$ along its span. The thickness of the beam is assumed to be small compared to the length so that the effects of rotary inertia and shearing deformation can be ignored. Provided that the attached inertia element is placed symmetrically with respect to the beam length and the beam is relatively short, e.g., the ratio of the beam length to width is <30, the beam's transverse motion can be considered to be purely planar [2]. It is further assumed that the peak amplitude of vibration may reach a certain relatively large value (i.e., of the order of beam length for the lower modes) but the slope of the elastica may not have a tangent perpendicular to the x-axis, i.e., θ may not be equal to $\pm 90^\circ$; also the beam is assumed to be conservative. These assumptions are the same as those used in references [1, 13] in studying the planar non-linear vibrations of a cantilever beam systems similar to the one under consideration. In this next subsection, following the analysis presented in reference [1], a Galerkin–Lagrange approach is used to derive a single mode non-linear temporal equation of motion of the beam.

2.2. EQUATION OF MOTION

In terms of the co-ordinate system shown in Figure 1, the potential energy V, due to bending, of the beam is given by

$$V = (EIl/2)\int_0^1 R^2(\xi, t)\,\mathrm{d}\xi, \tag{1}$$

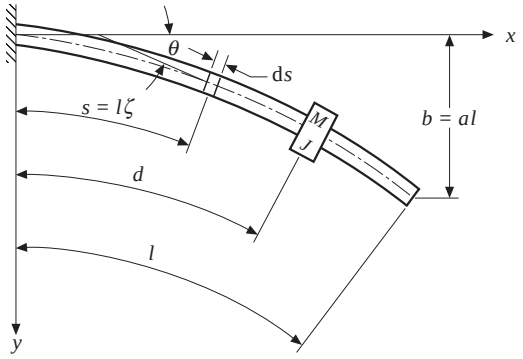

Figure 1. Sketch of the beam system under study.

where $\xi = s/l$ is a dimensionless arc length, EI is the modulus of flexural rigidity, and $R(\xi, t)$ is the radius of curvature of the beam neutral axis. In terms of the variables x, y, the exact radius of curvature R takes the form [13]

$$R = \lambda^3(x'y'' - x''y'), \tag{2}$$

where $\lambda = 1/l$ and a prime denotes differentiation with respect to the dimensionless arc length ξ. Equation (2), and thus equation (1), can be expressed in terms of only one variable, y, by noting that the variables x and y are related by the subsidiary relation [13]

$$x'^2 + y'^2 = l^2. \tag{3}$$

Then, by using equation (3) and its derivative with respect to ξ to eliminate x' and x'' from equation (2), and substituting the result into equation (1), one obtains

$$V = (EI\lambda^3/2)\int_0^1 (1 - \lambda^2 y'^2)^{-1}[(1 - \lambda^2 y'^2)y'' + \lambda^2 y'^2 y'']^2 \, \mathrm{d}\xi. \tag{4}$$

Noting, from equation (3), that $(\lambda y')^2 < 1$, upon expanding the term $(1 - \lambda^2 y'^2)^{-1}$ into a power series, equation (4), with non-linear terms retained up to fourth order, becomes

$$V = (EI\lambda^3/2)\int_0^1 [y''^2 + (\lambda y' y'')^2] \, \mathrm{d}\xi. \tag{5}$$

Next the kinetic energy T of the beam is presented and then is expressed in terms of only the variable y and its derivatives. With account taken of the axial and transverse inertia terms and the inertias of the attached element, the kinetic energy T of the beam in Figure 1 is given by

$$T = (ml/2)\int_0^1 (\dot{x}^2 + \dot{y}^2) \, \mathrm{d}\xi + \tfrac{1}{2}M(\dot{x}^2 + \dot{y}^2)|_{\eta l} + \tfrac{1}{2}J\dot{\theta}^2|_{\eta l}, \tag{6}$$

where a dot denotes a differentiation with respect to time t, $\eta = d/l$ is the dimensionless relative position parameter of the attached inertia element, and θ is the slope of the elastica and is given by [2]

$$\sin\theta = \mathrm{d}y/\mathrm{d}s = \lambda y', \tag{7}$$

where, as before, a prime denotes a differentation with respect to the dimensionless arc length ξ. Substituting the trigonometric identity $\cos^2\theta = 1 - \sin^2\theta$ into equation (7), and differentiating the result with respect to time t, one obtains

$$\dot{\theta}^2 = (\lambda \dot{y}')^2[1 - (\lambda y')^2]^{-1}. \tag{8}$$

Expanding the square bracketed term in the right side of equation (8) into a power series, and retaining non-linear terms up to fourth order, leads to

$$T = (ml/2)\int_0^1 (\dot{x}^2 + \dot{y}^2) \, \mathrm{d}\xi + \tfrac{1}{2}M(\dot{x}^2 + \dot{y}^2)|_{\eta l} + \tfrac{1}{2}J[(\lambda \dot{y}')^2 + (\lambda^2 \dot{y}' y')^2]_{\eta l}. \tag{9}$$

Next, it is noted that the beam consideration is assumed to be inextensible, which implies that the length of beam neutral axis remains constant during the motion. This imposes the constant relation [14]

$$(1 + \lambda x')^2 + (\lambda y')^2 = 1. \tag{10}$$

Rewriting equation (10) as

$$1 + \lambda x' = [1 - (\lambda y')^2]^{1/2}, \tag{11}$$

noting that $(\lambda y')^2 < 1$, expanding the right side of equation (11) into power series, retaining non-linear terms up to fourth order, and integrating the result from 0 to an arbitrary value of ξ, one obtains

$$x = \frac{-1}{2} \int_0^{\xi} (\lambda y'^2 + \tfrac{1}{4}\lambda^3 y'^4)\, \mathrm{d}\chi \tag{12}$$

Differentiating equation (12) with respect to time t leads to

$$\dot{x} = \frac{-1}{2} \left[\int_0^{\xi} (\lambda y'^2 + \tfrac{1}{4}\lambda^3 y'^4) \mathrm{d}\chi \right]^{\cdot}, \tag{13}$$

or

$$\dot{x}^2 = \frac{1}{4} \left[\left(\int_0^{\xi} \lambda y'^2 \, \mathrm{d}\chi \right)^{\cdot} \right]^2, \tag{14}$$

where non-linear terms of order greater than four are ignored. Upon substituting equation (14) into equation (9), the kinetic energy T of the beam becomes

$$T = (ml/2) \int_0^1 \left[\dot{y}^2 + \frac{1}{4} \left[\left(\int_0^{\xi} \lambda y'^2 \, \mathrm{d}\chi \right)^{\cdot} \right]^2 \mathrm{d}\xi + \frac{1}{2} M \left[\dot{y}^2 + \frac{1}{4} \left[\left(\int_0^{\xi} \lambda y'^2 \, \mathrm{d}\chi \right)^{\cdot} \right]^2 \right]_{nl} \right.$$
$$\left. + \frac{1}{2} \lambda^2 J [\dot{y}'^2 + (\lambda \dot{y}' y')^2]_{nl}. \right. \tag{15}$$

Using equations (5) and (15) one obtains, after factoring out the term $ml/2$, the beam's one-dimensional, Lagrangian L, $L = T - V$, as

$$L = (ml/2) \left\{ \int_0^1 \left[\dot{y}^2 + \frac{1}{4} \left(\left[\int_0^{\xi} \lambda y'^2 \, \mathrm{d}\chi \right]^{\cdot} \right)^2 \right] \mathrm{d}\xi + a_2 \left[\dot{y}^2 + \frac{1}{4} \left(\left[\int_0^{\xi} \lambda y'^2 \, \mathrm{d}\chi \right]^{\cdot} \right)^2 \right] \right\|_{nl}$$
$$+ a_1 [\dot{y}'^2 + (\lambda \dot{y}' y')^2]|_{nl} - \beta^2 \int_0^1 [y''^2 + (\lambda \dot{y}' y'')^2 \, \mathrm{d}\xi \Big\}, \tag{16}$$

where $a_1 = J\lambda^3/m$, and $a_2 = M\lambda/m$ are dimensionless inertia parameters of the attached inertia element with mass M and rotary inertia J, and $\beta^2 = EI\lambda^4/m$. It is to be noted that, if desired, one may apply Hamilton's principle, after integrating some of the terms in equation (16), to obtain the integro-partial differential field equation of motion and the corresponding boundary conditions. The interest in this work, however, is to obtain an approximate, single mode, ordinary differential equation in time t by using the assumed deflection mode method. Therefore, one can avoid the step of derivation of the

integro–partial differential field equation and instead use any of the variational procedures, i.e., Rayleigh–Ritz or Galerkin's procedure, to discretize the Lagrangian L in equation (16), and then apply the Euler–Lagrange equation to obtain the discrete temporal problem. Accordingly an approximate, single-mode solution is assumed to be of the form

$$y(\xi, t) = \phi(\xi)u(t), \tag{17}$$

where $\phi(\xi)$ is a normalized mode shape defection, to be determined later (in section 2.3), which is assumed to remain self-similar (i.e., independent of motion amplitude) during motion, and $u(t)$ is an unknown time modulation of the assumed deflection mode. Substituting equation (17) into equation (16), one obtains the discrete, single-mode (single co-ordinate), beam Lagrangian

$$L = (ml/2)\,[\alpha_1 \dot{u}^2 + \alpha_3 \lambda^2 \dot{u}^2 u^2 - \beta^2 \alpha_2 u^2 - \beta^2 \alpha_4 \lambda^2 u^4], \tag{18}$$

where

$$\alpha_1 = \int_0^1 \phi^2 \,\mathrm{d}\xi + a_1 \phi'^2(\eta) + a_2 \phi^2(\eta), \qquad \alpha_2 = \int_0^1 \phi''^2 \,\mathrm{d}\xi,$$

$$\alpha_3 = \int_0^1 \left(\int_0^\xi \phi'^2 \,\mathrm{d}\chi \right)^2 \mathrm{d}\xi + a_1 \phi'^4(\eta) + a_2 \left(\int_0^\xi \phi'^2 \,\mathrm{d}\chi \right)^2 |_n, \qquad \alpha_4 = \int_0^1 \phi'^2 \phi''^2 \,\mathrm{d}\xi. \tag{19}$$

Upon application of the Euler–Lagrange equation,

$$(\mathrm{d}/\mathrm{d}t)/(\partial L/\partial \dot{u}) - \partial L/\partial u = 0, \tag{20}$$

to the Lagrangian L in equation (18), one obtains, ignoring the multiplication constant ml, the discrete, single-mode, of order three non-linearities, beam temporal problem:

$$\alpha_1 \ddot{u} + \beta^2 \alpha_2 u + \alpha_3 \lambda^2 u^2 \ddot{u} + \alpha_3 \lambda^2 u \dot{u}^2 + 2\beta^2 \alpha_4 u^3 = 0. \tag{21}$$

It is to be noted that some of the coefficients α_i in equation (21), defined by equations (19), in general, as will be shown in section 2.4, increase sharply and attain relatively large values at the higher modes of the beam. Therefore, for convenience, equation (21) is scaled and converted to the dimensionless form

$$\ddot{q} + q + \varepsilon_1 q^2 \ddot{q} + \varepsilon_1 \dot{q}^2 q + \varepsilon_2 q^3 = 0, \tag{22}$$

where

$$\varepsilon_1 = \alpha_3/(p^2 \alpha_1), \qquad \varepsilon_2 = 2\alpha_4/(p^2 \alpha_2), \tag{23}$$

dots are now derivatives with respect to the dimensionless time $\tau = \beta(\alpha_2/\alpha_1)^{1/2} t$, $q = pu/l$ is the dimensionless displacement amplitude at the point of maximum deflection, and $p^2 = \Omega/\beta$ is the dimensionless frequency, and Ω is the frequency, of the assumed mode of the associated linear beam. The first two of the three non-linear terms in equation (22) which are inertia type due to kinetic energy of axial motion, arise as a result of using the inextensibility condition given by equation (10). The first of these two non-linear terms has a softening effect, while the second has a hardening effect [10]. The last of the three non-linear terms in equation (22) is a hardening static type due to potential energy stored in bending. It is to be noted that the present scaling procedure, which is similar to those used in references [1, 3], makes no prior assumption regarding the relative order of magnitude of various terms in equation (21). In particular, the arbitrary choice of the dimensionless linear frequency parameter p in the definition of the displacement scaling

factor is done for numerical convenience, so that the coefficients ε_1 and ε_2 in equation (22) would not attain numerically large values for the higher modes: i.e., this scaling procedure does not change the relative order of magnitude of the various terms in the original equation of motion.

2.3. THE LINEAR PROBLEM

In the derivation of the approximate non-linear equation (22), describing the temporal behavior of the beam vibration, one assumes the beam defection shape $\phi(\xi)$ to be a specified, self-similar (i.e., independent of motion amplitude), spatial function. This function, which must at least satisfy the beam boundary natural conditions, i.e., must at least be an admissible function, is taken, in this work, to be the eigenfunction (comparison function) of the associated linear beam which satisfies the associated linear beam equation of motion and all of its specified boundary conditions. In this case, the discretization procedure in section 2.2 is generally referred to as Galerkin's method, and when applied to the present beam problem requires that the function ϕ be a solution of the associated linear problem [11]:

$$y_1''''(\xi_1) - p^4 y_1(\xi_1) = 0, \qquad 0 \leqslant \xi_1 \leqslant \eta, \tag{24}$$

$$y_2''''(\xi_2) - p^4 y_2(\xi_2) = 0, \qquad 0 \leqslant \xi_2 \leqslant 1 - \eta, \tag{25}$$

subject to the following boundary and continuity conditions:

$$\text{at } \xi_1 = 0: \quad y_1 = 0, y_1' = 0; \qquad \text{at } \xi_1 = \eta, \xi_2 = 0: \quad y_1 = y_2, y_1' = y_2',$$

$$EI(y_1'' - y_2'') = J\Omega^2 l y_1', \qquad EI(y_1''' - y_2''') = -\Omega^2 l^3 M y_1;$$

$$\text{at } \xi_2 = 1 - \eta: \quad y_2'' = 0, y_2''' = 0. \tag{26}$$

Here $\xi_1 = s_1/l$, $\xi_2 = s_2/l$, s_1 and s_2 are arc lengths on the left and right sections of the beam, $p^4 = m\Omega^2 l^4/(EI)$ is a dimensionless frequency constant, Ω^2 is a natural frequency of the linear beam, and y_1 and y_2 are the deflections of the centerlines of the left and right sections of the beam. Note that the above linear problem formulation is restricted to the cases where $\eta < 1$; that is, the attached element cannot be placed at the tip of the beam. Also note that the clamped–free boundary conditions in equation (26) are formulated in terms of arc lengths s_i. These boundary conditions are formally the same as those formulated in terms of horizontal co-ordinates x_i in the classical linear beam theory [13]. This, however, is not true for the matching boundary conditions in these equations, which are assumed here to be the same as those formulated in terms of the horizontal co-ordinates x_i in the classical linear theory. The general solutions of the ordinary differential equations (24) and (25) are, respectively,

$$y_1(\xi_1) = C_1 \sin(p\xi_1) + C_2 \cos(p\xi_1) + C_3 \sinh(p\xi_1) + C_4 \cosh(p\xi_1), \tag{27}$$

$$y_2(\xi_1) = C_5 \sin(p\xi_2) + C_6 \cos(p\xi_2) + C_7 \sinh(p\xi_2) + C_8 \cosh(p\xi_2), \tag{28}$$

where C_i, $(i = 1, 2, \ldots, 8)$, are arbitrary constants to be determined by using the eight boundary and matching conditions given by equations (26). Upon substituting equations (27) and (28) into equations (26) one obtains a set of eight homogeneous algebraic equations for the eight unknown constants C_i. This set of equations, in matrix form, becomes

$$[d_{ij}]\{C\} = 0 \tag{29}$$

where $[d_{ij}]$ is an 8×8 coefficient matrix having the non-zero elements

$$
\begin{aligned}
&d_{12} = 1 && d_{14} = 1 && d_{21} = p && d_{23} = p \\
&d_{31} = sn && d_{32} = cn && d_{33} = sh && d_{34} = ch \\
&d_{36} = -1 && d_{38} = -1 && d_{41} = pcn && d_{42} = -psn \\
&d_{43} = pch && d_{44} = psh && d_{45} = -p && d_{47} = -p \\
&d_{51} = -p^2sn - 8p^5cn && d_{52} = 8p^5sn - p^2cn && d_{53} = p^2sh - 8p^5ch && d_{54} = p^2ch - 8p^5sh \\
&d_{56} = p^2 && d_{58} = -p^2 && d_{61} = a_2p^4sn - p^3cn && d_{62} = p^3sn + a_2p^4cn \\
&d_{63} = p^3ch + a_2p^4sh && d_{64} = p^3sh + a_2p^4ch && d_{65} = p^3 && d_{67} = -p^3 \\
&d_{75} = -p^2sn' && d_{76} = -p^2cn' && d_{77} = p^2sh' && d_{78} = p^2ch^2 \\
&d_{85} = -p^3cn' && d_{86} = p^3sn' && d_{87} = p^3ch' && d_{88} = p^3sh', \qquad (30)
\end{aligned}
$$

where $sn = \sin(p\eta)$, $cn = \cos(p\eta)$, $sh = \sinh(p\eta)$, $ch = \cosh(p\eta)$, $sn' = \sin(p(1-\eta))$, $cn' = \cos(p(1-\eta))$, $sh' = \sinh(p(1-\eta))$, $ch' = \cosh(p(1-\eta))$, and $a_1 = J\lambda^3/m$ and $a_2 = M\lambda/m$ are, as before, the inertia ratios of the attached element of mass M and rotary inertia J located at the relative position η. A non-trivial solution of the matrix characteristic equation (29) is possible only when the determinant of the coefficients matrix $|d_{ij}|$ vanishes. For a given set of parameter values a_1, a_2, and η, the non-trivial solutions of equation (29) are obtained in this work numerically by using, first, a LU decomposition scheme to find the characteristic determinant equation $|d_{ij}| = 0$, then a *regula–falsi* is used to find the first four roots, to the sixth decimal accuracy, of this characteristic equation: that is, the first four dimensionless frequency parameters p_i. The mode shape function ϕ_i corresponding to a root p_i is then found by using a back-substitution procedure to solve the first seven of equations (29) for the first seven constants C_i in equations (27) and (28) in terms of C_8. This yields the mode shape function ϕ_i as

$$\phi_i = [y_1(p_i\xi_1) + y_2(p_i\xi_2)]/C_8. \qquad (31)$$

Each mode shape function ϕ_i was then normalized so that it has a unity maximum value. In order to check the accuracy of the above numerical procedure, and due to lack of data in the technical literature, the first four frequency parameters p_i obtained by using the present procedure were compared with those available in references [11, 12] for various degenerate cases. The agreement between the various results was exact. For example, for $a_1 = a_2 = 0$, the present procedure yielded $p_1 = 1{\cdot}875104$, $p_2 = 4{\cdot}694091$, $p_3 = 7{\cdot}854757$, $p_4 = 10{\cdot}995541$; and for $a_1 = 0$, $a_2 = 0{\cdot}5$, $\eta = 0{\cdot}5$, the present procedure yielded $p_1 = 1{\cdot}581490$, $p_2 = 3{\cdot}539601$, $p_3 = 7{\cdot}853520$, $p_4 = 9{\cdot}612364$; these two sets of results where in exact agreement with those in references [11, 12]. Examples of the first four normalized mode shape functions ϕ_i obtained by using equation (31) for different sets of values of the parameters a_1, a_2 and η are shown in Figures 2(a–d). For example, for $a_1 = 0{\cdot}2$, $a_2 = 1$, $\eta = 0{\cdot}7$, the calculated values for the normalized third mode were: $p_3 = 6{\cdot}482103$, $C_1 = -0{\cdot}101291$, $C_2 = 0{\cdot}104381$, $C_3 = 0{\cdot}101291$, $C_4 = -0.104381$, $C_5 = 0{\cdot}327511$, $C_6 = -0{\cdot}541091$, $C_7 = -0{\cdot}350373$, and $C_8 = 0{\cdot}477193$. Figures 2(a–d) and those given in reference [11], as well as others not shown, indicate that mode shapes of the present beam, especially the second and higher ones, tend to change rapidly with respect to those of the base beam (i.e., with respect to the mode shapes shown in Figure 2(a) for which $a_1 = a_2 = 0$), as the intermediate inertia parameters a_1 and/or a_2 become relatively large. The normalized exact linear mode shape function ϕ_i, equation (31), and its derivatives were used in equations (19), along with equation (23), to calculate the parameters ε_1 and ε_2 in

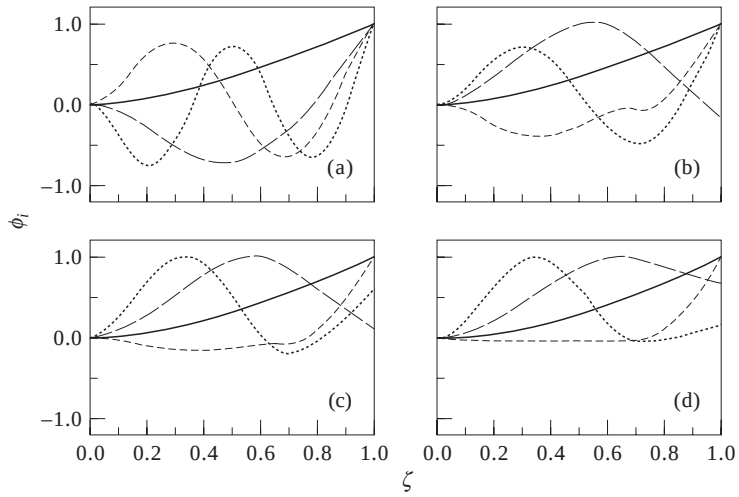

Figure 2. First four modes ϕ_i for the following cases: (a) $a_1 = a_2 = 0$; (b) $a_1 = 0{\cdot}5$, $a_2 = 0{\cdot}1$, $\eta = 0{\cdot}7$; (c) $a_1 = 0{\cdot}2$, $a_2 = 1{\cdot}0$, $\eta = 0{\cdot}7$; (d) $a_1 = 2{\cdot}0$, $a_2 = 5{\cdot}0$, $\eta = 0{\cdot}7$. ———, ϕ_i; — —, ϕ_2; - - - -, ϕ_3; ·····, ϕ_4.

the single-mode non-linear temporal problem given by equation (22). For given a_1, a_2 and η, the parameters ε_1 and ε_2 were calculated for each of the first four modes. The integrals in equations (19) defining the coefficients α_i were evaluated numerically by using Simpson's rule with an integration step size $\xi = 0{\cdot}001$, after using a symbolic manipulator program, called Derive, to evaluate the integral $(\int_0^\xi \phi'^2 \, d\chi)^2$ in the third of these equations. Following is a sample of the results obtained for the third mode of the case shown in Figure 2(c) for which $a_1 = 0{\cdot}2$, $a_2 = 1$, $\eta = 0{\cdot}7$ and $p = p_3 = 6{\cdot}482103$. The results were $\alpha_1 = -0{\cdot}087691$, $\alpha_2 = 154{\cdot}817$, $\alpha_3 = 1{\cdot}39593$, $\alpha_4 = 729.064$, $\varepsilon_1 = 0{\cdot}378861$, and $\varepsilon_2 = 0{\cdot}224154$.

Table 1 shows the values of ε_1 and ε_2 for each of the first four modes of the four cases given in Figures 2(a–d) when using the exact linear ϕ_i. For each case, Table 1 also shows, for comparison purposes, the values of ε_1 and ε_2 obtained by using the corresponding base beam linear mode shape shown in Figure 2(a). These results, and others not shown, indicate that, in general, when the inertia parameters a_1 and/or a_2 of the attached element are not relatively small, the values of the parameters ε_1 and/or ε_2, depending on the relative position η of the attached element, obtained by using the exact linear mode shape can be significantly different from those obtained by using the corresponding base beam linear mode. It is to be noted again, that in the present beam model in equation (22) one assumes the beam deflection to remain self-similar during the motion, i.e., to be amplitude independent, even when the motion amplitude is relatively large. In reality, however, one expects the deflection of the present non-linear beam at relatively large motion amplitudes to become amplitude dependent and, thus, it may deviate significantly from the assumed linear mode. Hamdan and Shabaneh [1] have shown that, in some cases, small variations, i.e., variations in the range shown in Table 1, in the values of ε_1 and ε_2 can lead not only to appreciable quantitative, but also qualitative, errors in period–amplitude behavior for the free response of the nonlinear oscillator in equation (22), even when ε_1 and ε_2 are not large compared to unity. Based on these results, and those shown in Table 1, one may question the accuracy of using an assumed linear mode method, which is a frequently used method in the analysis of non-linear continuous systems, to approximate the large amplitude non-linear behavior of the present beam system. It is hoped, however, that the results of the present model may be used for comparison purposes. Approximate

analytic and numerical solutions for the non-linear oscillator in equation (22), representing the temporal behavior of the present non-linear beam are presented in the next section.

3. APPROXIMATE ANALYTIC SOLUTIONS

The sample calculations of the parameters ε_i in equation (22), presented in Table 1, indicate that, for the range of amplitudes to be considered in this work (u/l up to 0·8 for the first mode and up to 0·4 for the fourth mode, $q = pu/l$), the non-linear conservative autonomous oscillator described by this equation is in general strongly non-linear, specially for the second and higher modes. Therefore, an approximate analytic solution for this oscillator obtained by using small perturbation methods will not be adequate for the range of large amplitude vibrations to be considered in this work, as these methods are restricted to the solution for weakly non-linear oscillators; e.g., when the amplitude of vibration is restricted to values for which the non-linear terms in equation (22) remain small (in this case less than unity) compared to the linear ones. In the current work, as was indicated in section 1, the HB method is used to obtain approximate solutions to equation (22). Single-term harmonic balance (STHB), and two-terms harmonic balance (2THB) approximate analytic solutions are presented and compared with those obtained by numerically integrating equation (22). Without loss of generality, the initial conditions are taken to be $q(0) = B$, $\dot{q}(0) = 0$ where B is the amplitude of motion. Note that $\phi_{max} = 1$,

TABLE 1

Values of system parameters ε_1 and ε_2 in equation (22) for the first four modes obtained by using the exact and base beam mode shapes for selected combinations of beam parameters

			Exact ϕ_i			Base Beam ϕ_i	
η	a_1	a_2	p_i	ε_1	ε_2	ε_1	ε_2
–	0·00	0·00	1·875104	0·326976	0·233241	0·326976	0·233241
			4·694090	1·651841	0·316578	1·651841	0·316578
			7·854759	4·103424	0·285887	4·103424	0·285887
			10·995577	8·381424	0·278835	8·381424	0·278835
0·70	0·05	0·10	1·691659	0·780287	0·330497	0·574519	0·233241
			3·483086	2·067569	0·443412	1·570166	0·316578
			6·816454	0·464160	0·150334	3·424372	0·285887
			7·587792	2·791904	0·245193	1·811038	0·278835
0·70	0·20	1·00	1·334241	2·889322	0·569997	1·200419	0·233241
			2·626170	3·314534	0·550754	2·863996	0·316578
			6·482103	0·378861	0·224154	1·450075	0·285887
			6·974931	2·614042	0·218520	2·048299	0·278835
0·70	1·00	1·00	1·038512	3·432908	1·260486	0·783540	0·233241
			2·282654	0·236845	0·392351	1·045432	0·316578
			6·416185	0·395492	0·226895	1·267895	0·285887
			6·970787	2·635984	0·220440	0·675209	0·278835
0·70	2·00	5·00	0·847512	7·476456	1·734567	1·135901	0·233241
			1·715321	0·473561	0·703051	1·781517	0·316578
			6·307206	0·345341	0·238802	0·385541	0·285887
			6·801119	2·153222	0·205214	1·108322	0·278835

and $\phi'_{max} \simeq p\phi_{max} = p$, and then from equation (17), $\lambda y'_{max} = p\phi'_{max}\lambda u_{max} \simeq pa_{max}$, so that the restriction $|\lambda y'| < 1$ used in section 2.2 implies that $a_{max} \simeq 1/p$.

3.1. SINGLE-TERM HARMONIC BALANCE (STHB) SOLUTION

According to the STHB method, with $q(0) = B$, $\dot{q}(0) = 0$, an approximate solution of equation (22) is written as

$$q(\tau) = B\cos\omega\tau, \tag{32}$$

where B is the amplitude and ω is the frequency of motion. Substituting equation (32) and its derivatives into equation (22), using the trigonometric identities $\cos^3\omega\tau = \frac{1}{4}(3\cos\omega\tau + \cos 3\omega\tau)$, $\sin^2\omega\tau = 1 - \cos^2\omega\tau$, and collecting the $\cos\omega\tau$ and $\cos 3\omega\tau$ terms, one obtains

$$[1 + \tfrac{3}{4}\varepsilon_2 B^2 - \omega^2(1 + (\varepsilon_1/2)B^2)]\cos\omega\tau + (\varepsilon_2/4 - (\varepsilon_1/2)B^2\omega^2)\cos 3\omega\tau = 0. \tag{33}$$

Upon ignoring the effect of the third harmonic $\cos 3\omega\tau$, and setting the coefficient of $\cos\omega t$ to zero, one obtains the following non-linear frequency–amplitude relation

$$\omega^2 = (1 + \tfrac{3}{4}\varepsilon_2 B^2)\,(1 + (\varepsilon_1/2)B^2)^{-1}. \tag{34}$$

The period v of motion, in terms of the dimensionless time $\tau = \beta(\alpha_2/\alpha_1)^{1/2}t$, is then obtained by substituting $v = 2\pi/\omega$ into equation (34), which yields

$$v = 2\pi(1 + (\varepsilon_1/2)B^2)^{1/2}(1 + \tfrac{3}{4}\varepsilon_2 B^2)^{-1/2}. \tag{35}$$

For convenience, equation (35) is rewritten in terms of the dimensionless time βt and the dimensionless displacement amplitude $a = b/l = B/p$ (recall that $q = pu/l$, where p is the linear mode eigenfrequency parameter) so that the period T of motion becomes

$$T = 2\pi(\alpha_1/\alpha_2)^{1/2}[1 + (\varepsilon_1/2)\,(ap)^2]^{1/2}[1 + \tfrac{3}{4}\varepsilon_2(ap)^2]^{-1/2}. \tag{36}$$

The non-linear period amplitude relation in equation (36) represents the first order approximation which one also obtained using classical perturbation methods. It can be seen from this equation that for the cases where ε_1 and ε_2 are not small compared to 1, the period T becomes nearly constant independent of the motion amplitude a: i.e., $T \to 2\pi(1{\cdot}5\varepsilon_2/\varepsilon_1)^{-1/2}$, as the amplitude of motion becomes of order, or greater than, $1/p$. For the cantilever beam under consideration, the dimensionless linear frequency parameter p increases rapidly as the mode index is increased: i.e., for the case $a_1 = a_2 = 0$, $p = 1{\cdot}875104$ for the first mode, and $p = 10{\cdot}995541$ for the fourth mode. Thus the above limiting value of amplitude a at, and above, which the period T becomes nearly a constant independent of motion amplitude a decreases rapidly as the mode index is increased. Also note that, by setting the left side of equation (36) equal to 2π, the non-linear period T, according to equation (36), becomes equal to the linear period and is independent of the motion amplitude a for all values of a whenever $(\epsilon_1/\epsilon_2) = 1{\cdot}5$. This result also indicates that the period T of the oscillator in equation (22) exhibits a softening behavior, i.e., the period T increases with increasing amplitude a, when $(\varepsilon_1/\varepsilon_2) > 1{\cdot}5$, and a hardening behavior, i.e., T decreases with increasing a, when $(\varepsilon_1/\varepsilon_2) < 1{\cdot}5$. Results obtained from equation (36), for various selected values of system parameters a_1, a_2 and η, are, for convenience, presented and discussed in the next section.

3.2. TWO-TERMS HARMONIC BALANCE (2THB) SOLUTION

In order to improve the accuracy of the STHB solution, one adds more harmonics to the assumed STHB solution. When the number of different harmonics in the assumed solution is equal to two, the HB method is called the two-terms harmonic balance (2THB)

method. According to this method, with $q(0) = B$, $\dot{q}(0) = 0$, one assumes an approximate solution to equation (22) in the form

$$q(\tau) = B_1 \cos \omega\tau + B_3 \cos 3\omega\tau, \tag{37}$$

where

$$B = B_1 + B_3. \tag{38}$$

Equation (38) relates the total amplitude B of motion to the amplitudes B_1 and B_3 of the response fundamental and third harmonics, respectively. Upon substituting equation (37) and its derivatives into equation (22), using trigonometric identities, retaining only $\cos \omega\tau$ and $\cos 2\omega\tau$ terms, then equating the coefficient of each of these two harmonics to zero, one obtains the following two non-linear coupled algebraic equations:

$$B_3 = \left[0{\cdot}25\epsilon_1\left(B_1^3 + 3B_3^3\right) - 0{\cdot}5\epsilon_1\left(B_1^3 + 9B_3^3\right)\right] \Big/ \left[\vartheta\omega^2 - 1 - 1{\cdot}5\varepsilon_2 B_1^2 + 5\varepsilon_1\omega^2 B_1^2\right], \tag{39}$$

$$\omega^2 = \left(1 + 0{\cdot}75\varepsilon_2\left[B_1^2 + B_1 B_3 + 2B_3^2\right]\right) \Big/ \left(1 + 0{\cdot}5\varepsilon_1\left[B_1^2 + 3B_1 B_3 + 10B_3^2\right]\right). \tag{40}$$

Equations (39) and (40) along with equation (38), for a given amplitude B, define the amplitudes B_1 and B_3, respectively, of the fundamental and third harmonics, and the frequency of the assumed period of motion of the non-linear oscillator given by equation (22). These coupled non-linear equations were solved numerically by using a direct iterative procedure with 10^{-6} accuracy. The dimensionless motion amplitude $a = b/l$ is then calculated by noting that $B = pa$, and the period v of motion is calculated by using the relation $v = 2\pi/\omega$, which in the dimensionless time βt becomes

$$T = 2\pi(\alpha_1/\alpha_2)^{1/2}/\omega. \tag{41}$$

The dimensionless periods T, in βt time, calculated by using equations (38–41) for selected values of beam parameters a_1, a_2 and η are presented and discussed in the next section.

In additon to the above analytical solutions, equation (22) was also integrated numerically by using the fourth order Runge–Kutta method with integration step size $\Delta\tau = 10^{-3}$. Again, the initial conditions were taken to be $q(0) = B = pa$, $\dot{q}(0) = 0$, and the period T in βt time was obtained by multiplying the numerically calculated period by the scaling factor $(\alpha_1/\alpha_2)^{1/2}$.

4. RESULTS AND DISCUSSION

The dimensionless period T, in time βt, of each of the first four modes of free vibration of the cantilevered beam system shown in Figure 1 was calculated, for given values of inertia parameters a_1, a_2 and position of the attached element, analytically by using the STHB, equation (36), and 2THB, equations (38–41), and numerically by using the fourth order Runge–Kutta method. All of these calculations were programmed by using single precision on a VAX/VMS version 5 digital computer. Examples of the results of these calculations are shown in Figures (3–7), which display the non-linear period parameter T variation with the beam dimensionless peak displacement $a = (b/l) = B/p$ at the point of maximum deflection for various selected values of a_1, a_2 and η. The interest of this work is in the large amplitude free motions; therefore the calculations in each case where carried

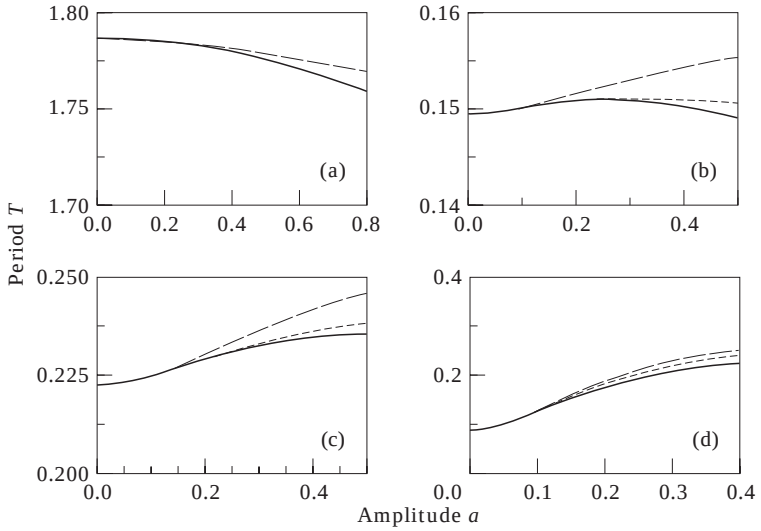

Figure 3. Comparisons of the SHB, 2THB and numerical results for the variation of the period T with amplitude a: (a) $a_1 = a_2 = 0$, $p = p_1$; (b) $a_1 = 0{\cdot}2$, $a_2 = 1{\cdot}0$, $\eta = 0{\cdot}7$, $p = p_3$; (c) $a_1 = 0{\cdot}1$, $a_2 = 0{\cdot}2$. $\eta = 0{\cdot}6$, $p = p_3$; (d) $a_1 = 0{\cdot}5$, $a_2 = 0{\cdot}2$, $\eta = 0{\cdot}6$, $p = p_4$. ———, Numerical; — —, SHB; ----, 2THB.

out for amplitude free motions; therefore the calculations in each case where carried out for amplitude a values up to 0·8 for the first mode and up to 0·4 for the fourth mode.

Figures 3(a–d) show comparisons between $T - a$ curves obtained by using the approximate STHB and 2THB analytic results and the numerical integration results, where the exact linear mode shape function ϕ was used in each case. The cases considered in these four figures are, respectively as follows: (a) $a_1 = a_2 = 0$, $p = p_1 = 1{\cdot}875104$ (i.e., first mode), where $\varepsilon_1 = 0{\cdot}326976$, $\varepsilon_2 = 0{\cdot}284413$, and thus $(\varepsilon_1/\varepsilon_2) = 1{\cdot}15 < 1{\cdot}5$; (b) $a_1 = 0{\cdot}2$, $a_2 = 1$, $\eta = 0{\cdot}7$, $p = p_3 = 6{\cdot}482103$ where $\varepsilon_1 = 0{\cdot}378861$, $\varepsilon_2 = 10{\cdot}224154$ which gives $(\varepsilon_1/\varepsilon_2) = 1{\cdot}71 < 1{\cdot}8$; (c) $a_1 = 0{\cdot}1$, $a_2 = 0{\cdot}2$, $\eta = 0{\cdot}6$, $p = p_3 = 5{\cdot}315102$ where $\varepsilon_1 = 0{\cdot}567745$, $\varepsilon_2 = 0{\cdot}275332$ and thus $(\varepsilon_1/\varepsilon_2) = 2{\cdot}062 > 1{\cdot}8$; (d) $a_1 = 0{\cdot}5$, $a_2 = 0{\cdot}2$, $\eta = 0{\cdot}6$, $p = p_4 = 8{\cdot}292397$, where $\varepsilon_1 = 4{\cdot}041788$, $\varepsilon_2 = 0{\cdot}243714$, and thus $(\varepsilon_1/\varepsilon_2) = 16{\cdot}584 \gg 1{\cdot}5$. These figures, and others not shown, as well as others shown in references [1, 10], indicate that

(1) when $(\varepsilon_1/\varepsilon_2) \gg 1{\cdot}5$ or $(\varepsilon_1/\varepsilon_2) \ll 1{\cdot}5$, the accuracy of the STHB solution is reasonably good for small, and fair for moderate, values of the dimensionless motion amplitude a, but becomes poor as a becomes relatively large, i.e., $0{\cdot}5 < a < 1$; while the accuracy of the 2THB solution is fairly good for moderate values of a, and becomes poor, but appreciably better than that of the STHB, for relatively large a. For given $\varepsilon_1/\varepsilon_2 \gg 1{\cdot}5$ or $\varepsilon_1/\varepsilon_2 \ll 1{\cdot}5$, the accuracy of the STHB and that of the 2THB is better when ε_1 and ε_2 are small compared to 1, i.e., when the system is weakly non-linear; also this accuracy is better when $\varepsilon_2 > \varepsilon_1$ than when $\varepsilon_2 < \varepsilon_1$;

(2) the accuracy of the STHB solution becomes poor, even for moderately small values of a, when $\varepsilon_1/\varepsilon_2$ approaches, from above or from below, the range $1{\cdot}5 < (\varepsilon_1/\varepsilon_2) < 1{\cdot}8$. When $\varepsilon_1/\varepsilon_2$ is, roughly, in this range, the STHB solution fails qualitatively, and perhaps quantitatively, as it incorrectly predicts a softening $T - a$ behavior, while the 2THB and numerical solution predict a hardening $T - a$ behavior (i.e., Figure 3(b)). It is to be noted that the 2THB solution can also fail to provide the correct qualitative $T - a$ behavior for the present beam model in equation (22); however, this failure occurs over an appreciably smaller subrange of the above range of the STHB solution;

(3) the analytic STHB and 2THB, and numerical solutions shown that, for each mode, the $T - a$ curve starts to level off: i.e., the period T becomes nearly a constant independent of the motion amplitude a, at relatively moderate values of A, where the value of a at which this leveling-off begins decreases when the ratio $\varepsilon_1/\varepsilon_2$ is increased, for $\varepsilon_1 \gg \varepsilon_2$, and when $\varepsilon_1/\varepsilon_2$ is decreased, for $\varepsilon_1 \ll \varepsilon_2$. Hamdan and Shabaneh [10] have shown that the $T - a$ curves of the non-linear conservative oscillator in equation (22) exhibit a softening behavior when, approximately, $\varepsilon_1/\varepsilon_2 > 1{\cdot}6$, and hardening type when $\varepsilon_1/\varepsilon_2 < 1{\cdot}6$. They also have shown that the period T becomes a constant independent of motion amplitude a for all values of a and equal to the linear period, i.e. $T = 2\pi$, when $(\varepsilon_1/\varepsilon_2) \sim 1{\cdot}6$. The values of system parameters a_1, a_2, η, for which this value of the ratio $\varepsilon_1/\varepsilon_2$ is obtained for a given mode can be calculated by a trial and error procedure and has not been done in this work. Note that this value of the ratio $\varepsilon_1/\varepsilon_2$ is not possible to obtain for a cantilever beam without an intermediate inertia element.

Figures 4(a–d), obtained numerically, show examples of the effects on the $T - a$ curves of using the base beam mode shape instead of the corresponding exact linear mode shape when the inertia parameters a_1 and/or a_2 of the attached element are not zero. The results in these figures, and others not shown, indicate that the use of an approximate mode shape can have a significant effect on the predicted $T - a$ behavior, especially when a_1 and/or a_2, depending on the relative position η of the attached element, are not small.

Figures 5(a–d), obtained numerically, show examples of the effect on the $T - a$ behavior of increasing the mass ratio parameter a_2 of the attached element mass M to beam mass. These results indicate that, in general, as in linear theory, increasing the mass of the attached element, for given relative position η and relative rotary inertia a_1 of the attached element, tends to increase the period of each of the modes of beam free vibration. These results also indicate that small changes in the mass ratio a_2 can lead to an appreciable change in the period T of each of the first modes, especially for the higher modes and at large motion amplitudes. It is to be noted that for the case $a_1 = a_2 = 0$, the $t - a$ curve exhibits a hardening behavior for the first mode, and a softening behavior for the second and higher modes. When a_1 and/or a_1 are not zero, the $T - a$ curve for the first mode and

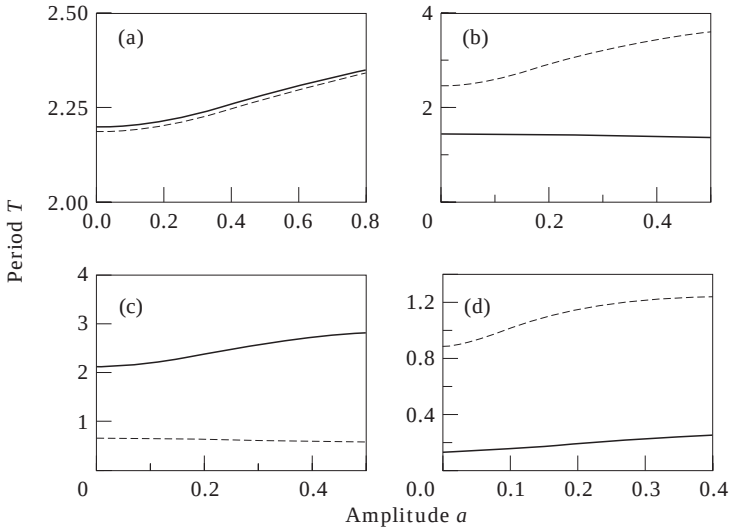

Figure 4. Effect of mode shape on the period T variation with amplitude a obtained numerically: (a) ϕ_1; $a_1 = 0{\cdot}05$; $a_2 = 0{\cdot}1$, $\eta = 0{\cdot}7$; (b) ϕ_2; $a_1 = a_2 = 1{\cdot}0$, $\eta = 0{\cdot}8$; (c) ϕ_3; $a_1 = a_2 = 1{\cdot}0$, $\eta = 0{\cdot}2$; (d) ϕ_4; $a_1 = 2{\cdot}0$, $a_2 = 5{\cdot}0$, $\eta = 0{\cdot}7$. ———, Exact; ----, approximate.

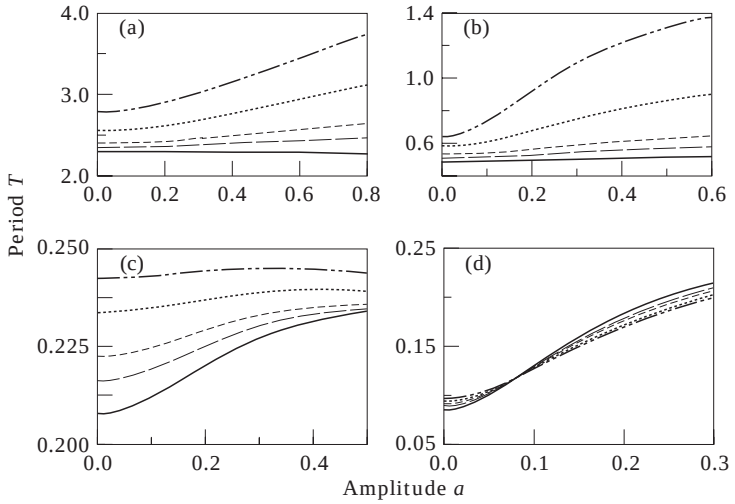

Figure 5. Effect of lumped mass parameter a_2 on the variation of period T with amplitude a when using exact ϕ_i for the case $a_1 = 0{\cdot}1$ and $\eta = 0{\cdot}6$. (a) ϕ_1; (b) ϕ_2; (c) ϕ_3; (d) ϕ_4. ———, $a_2 = 0{\cdot}0$; — —, $a_2 = 0{\cdot}1$; ----, $a_2 = 0{\cdot}2$; ·····, $a_2 = 0{\cdot}5$; —·—, $a_2 = 1{\cdot}0$.

the $T - a$ curve for the second mode each may exhibit a hardening or softening behavior, depending on the values of the inertias a_1, a_2 and position η of the attached element.

Figures 6(a–d), obtained numerically, show the examples of the effect of increasing the rotary inertia parameter a_1 of the attached element. These results indicate that, as in linear theory [11, 12], increasing the rotary inertia of the attached element tends to increase the period of motion for each of the modes of beam free vibration. These results also indicate that, depending on the position of the attached element, relatively small changes in the

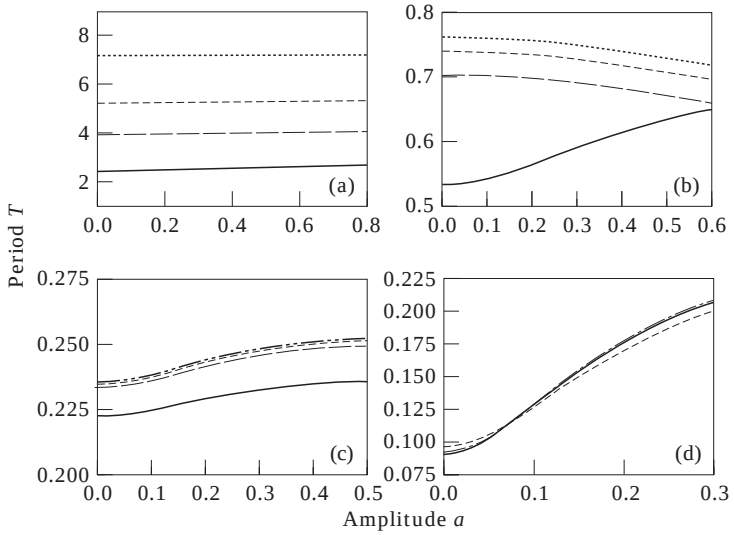

Figure 6. Effect of rotary inertia parameter a_1 on the variation of period T with amplitude a when using exact ϕ_i for the case $a_2 = 0{\cdot}2$ and $\eta = 0{\cdot}6$. (a) ϕ_1; (b) ϕ_2; (c) ϕ_3; (d) ϕ_4. ———, $a_1 = 0{\cdot}1$; — —, $a_1 = 0{\cdot}5$; ----, $a_1 = 1{\cdot}0$; · · ·, a_1, $= 2{\cdot}0$.

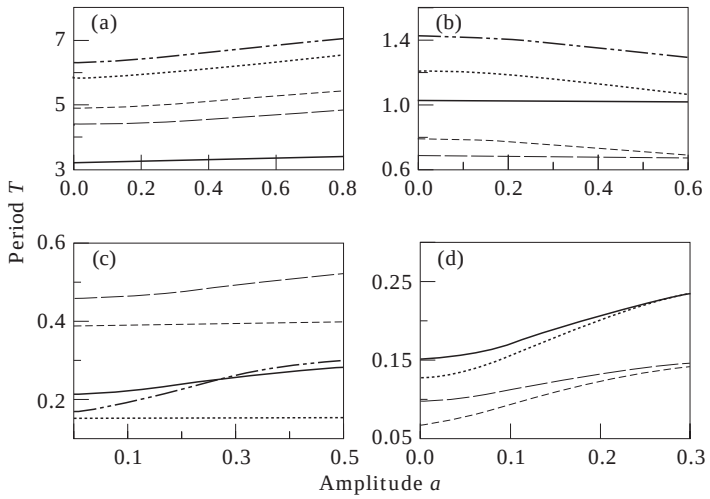

Figure 7. Effect of lumped mass position η on the variation of period T with amplitude a when using exact ϕ_i for the case $a_1 = a_2 = 1{\cdot}0$. (a) ϕ_1; (b) ϕ_2; (c) ϕ_3; (d) ϕ_4. ———, $\eta = 0{\cdot}2$; — —, $\eta = 0{\cdot}4$; ----, $\eta = 0{\cdot}5$; ·····, $\eta = 0{\cdot}7$; —··— , $\eta = 0{\cdot}8$.

rotary inertia ratio a_1 can lead to significant changes in the period T of each of the first four modes, especially when amplitude a of motion is not relatively small.

Figures 7(a–d), obtained numerically, show examples of the effect of changing the relative position η of the attached inertia element for the case $a_1 = a_2 = 1$. These results show that for the values of a_1, a_2 and η considered in these figures the $T - a$ curves of the first, third or fourth mode are of the softening type, while those of the second mode can be of the hardening or softening type depending on the relative position η of the attached inertia element. Note that, as indicated in the previous section and as was shown in reference [1] and other references, when $a_1 = a_2 = 0$, or $a_1 = 0$ and a_2 is small, i.e., when the inextensible cantilever beam does not carry an inertia element or carries an element having a relatively small mass and negligible rotary inertia, the $T - a$ curves for the first mode exhibit a hardening behavior, while those for the second and higher modes exhibit a softening behavior. One may conclude therefore, from the present results and from those in reference [1], that the $T - a$ curves for the first and second modes of the present beam can each be of the softening or hardening type depending on the inertias, in particular the rotary inertia, and position of the attached element. The present results, and those in reference [1], also indicate that, in general, moving the attached mass towards the clamped end of the beam tends to increase the period of the first mode and decrease that of the second, or higher, modes. However, as in linear theory [11,12], when the amplitude of motion is small, the period of the second, or higher, mode goes through regions of increasing and decreasing values as the attached mass is moved towards the clamped end of the beam. The present results, as well as those in reference [1], also indicate that, depending on the values of the inertia parameters a_1 and a_2 of the attached element, changing the position of the attached element can lead to relatively large changes in the period of free motion, especially when the amplitude of motion is relatively large.

5. CONCLUSIONS

The aims of the present work are to provide a simple formulation, by using well established analytical techniques, of the problem of large amplitude, planar, flexural free

vibrations of an inextensible beam carrying at an intermediate point along its span an element having, relatively, a small mass and a small rotary inertia, and to study the effects of the inertias and position of the attached element on the non-linear period of free motion of such a beam element. Applying the assumed single-mode method to the beam Lagrangian led directly to the non-linear ordinary differential equation describing the temporal behavior of the beam, single-mode, vibration, and thus avoided the derivation of the field integro–partial differential equation of motion and the associated boundary conditions. It is shown that the inertia non-linearities arise in this case as a result of the inextensibility of the beam. In the present analysis it is assumed that the non-linear frequencies of the beam, which are amplitude dependent, remain widely spaced, as are the linear ones, even when the amplitude of motion is relatively large. It is also assumed that the beam deflection during the motion resembles a linear mode shape of the beam and remains self-similar during the motion even when the amplitude of motion is large. These assumptions, although simplifying the calculations considerably, may introduce significant errors at large amplitudes especially when the ratio of the attached mass to the beam mass is not small. For example, it was shown that even when the mass and/or the rotary inertia of the attached element are not relatively large, the use of the base beam mode shape instead of the corresponding exact linear mode shape can lead to significant errors in the period of the response. It can also be seen from Figures (5–7) that, as in linear theory [11, 12], when the inertia parameters a_1 and/or a_2 of the attached element are not small, the frequencies of two consecutive modes are not as widely spaced as for the case when $a_1 = a_2 = 0$, and may become, depending on the relative position η of the attached element, very close to each other. In such cases, one may expect the beam vibration to occur at more than one mode simultaneously. The present results also show that the inertias and position of an attached element have similar effects on the period of the non-linear system as in linear theory when the amplitude of motion is small; but their effects are more pronounced than in linear theory when the amplitude of motion is relatively large.

REFERENCES

1. M. N. Hamden and N. H. Shabaneh 1997 *Journal of Sound and Vibration* **199**, 711–736. On the large amplitude free vibrations of a restrained uniform beam carrying an intermediate lumped mass.
2. L. D. Zavodney and A. H. Nayfeh 1989 *Intermediate Journal of Nonlinear Mechanics* **4**, 105–125. The nonlinear response of a slender beam carrying a lumped mass to a principal parametric excitation: theory and experiment.
3. T. D. Burton and M. Kolowith 1988 *Proceedings of the Second Conference on Nonlinear Vibrations*, *Stability*, *and Dynamics of Structures and Mechanisms*, *Blacksburg*, VA, 1–5. Nonlinear resonances and chaotic motion in a flexible parametrically excited beam.
4. T. J. Anderson, B. Balachandran and A. H. Nayfeh 1994 *American Society of Mechanical Engineers*, *Journal of Vibration and Acoustics* **116**, 480–484. Nonlinear resonances in a flexible cantilever beam.
5. R. M. Rosenberg 1961 *Applied Mechanics Reviews* **14**, 837–841. Nonlinear oscillations.
6. J. G. Eisley 1966 *Applied Mechanics Surveys*, *Spartan*, 285–290. Nonlinear deformation of elastic beams, rings and strings.
7. A. H. Nayfeh and T. D. Mook 1979 *Nonlinear Oscillations*. New York: John Wiley.
8. M. Sathyamoorthy 1982 *Shock and Vibration Digest* **14**, 19–35. Nonlinear analysis of beams part I: a survey of recent advances.
9. M. Sathyamoorthy 1982 *Shock and Vibration Digest* **14**. 7–18. Nonlinear analysis of beams part II: finite element methods.
10. M. N. Hamdan and N. H. Shabaneh 1997 *Journal of Sound and Vibration* **199**, 737–750. On the period of large amplitude free vibration of conservative autonomous oscillators with static and inertia type cubic non-linearities.

11. M. N. Hamdan and L. A. Latif 1994 *Journal of Sound and Vibration* **169**, 527–545. On the numerical convergence of discretization methods for the free vibrations of beams with attached inertia elements.
12. W. H. Liu and C.-C. Huang 1988 *Journal of Sound and Vibration* **123**, 31–42. Free vibration of restrained beam carrying concentrated masses.
13. H. Wagner 1965 *Transactions of the American Society of Mechanical Engineers*, *Journal of Applied Mechanics* **32**, 887–892. Large-amplitude free vibrations of a beam.
14. M. R. M. Crespo da Silva and C. C. Glynn 1978 *Journal of Structural Mechanics* **6**, 437–461. Nonlinear flexural-flexural-torsion dynamics of inextensional beam, I: equations of motion.